P-wave and S-wave near-surface characterization in Northeast British Columbia (NEBC)

Liliana Zuleta and Donald C. Lawton

ABSTRACT

A seismic survey in NEBC was acquired, using shear (SH) and compressional (P) sources and 3-component geophones. First break arrivals were picked in both data sets and the plus-minus time analysis method was used to calculate the depth and velocity of the layers that were detected with the offset of 1500 m used during the acquisition. The intent of this experiment was to gather all the required information in order to elucidate the near surface P and S-wave velocity-depth structure. This model will help in the processing of a 3D/3C seismic survey that will be acquired in this area, and to provide constraints on registration of PP and PS volumes.

From the P-V data, one refractor was detected and the presence of a channel was confirmed to the east end of the line. The depth of this refractor ranges from 140 m to ~230 m at the channel. The average velocity for the first layer is 1950 m/s and for the second layer is 2800 m/s. From the S-wave data a different model was determined, with two refractors detected to the west and only one refractor to the east. The depth of the first refractor is ~70 m and the second ~140 m; to the east the refractor detected is at ~180 m. The velocity for the first layer is 350 m/s to 420 m/s, and 500 m/s to 680 m/s for the second layer to the west and 1400 m/s for the third layer to the west. At the east end the velocity of the second layer is 1100 m/s. Finally the static correction times were computed. For SH data the static times is from -160 ms to -330 ms and for the P data, values ranging from -10 ms to -28 ms are obtained. A comparison with the generalized linear inversion (GLI) method was also made.

INTRODUCTION

Shear and compressional data have been used before for near surface characterization in order to calculate static corrections (Al Dulaijan, 2008; Martin, 2002; Parry and Lawton, 1993). Static corrections are used in the processing of reflection seismic data to remove the effect of low velocity in the shallow layer and the effects of elevation. The problem with statics is more severe in areas with glacial sediments due to its irregular thickness, which is the case in most of western Canada (Lawton, 1990) and therefore in Northeast British Columbia.

The main objective of this study is to obtain accurate depth and velocities in order to have a detailed description of the near-surface structure. For this report, only an east-west segment from the seismic survey was used for the analysis. This section comprised 220 shots. Two datasets were used; the vertical data (P) which was the result of P-wave source recorded on the vertical component and the shear data (S) which was the result of the shear vibrator on one of the horizontal components of the geophone. The shear vibrator was vibrating transverse to the line, as a result the data used was the one acquired in the transverse component because it showed more first arrival energy. Rotation of the original data was performed to transform it into radial and transverse

components. The field orientation of the H_2 component of the geophones was zero degrees (magnetic north). After rotation of the data, the first break arrivals were picked in VISTA software and these values were exported for the plus-minus analysis. Two methodologies were used: Manual calculation with Excel spreadsheets and a digital program coded in Fortran. Depth and velocities were obtained and from them static corrections were calculated.

Theory (Rotation and Plus-Minus method)

Rotation

Shear waves can be described in terms of the direction of propagation (polarization) relative to source-receiver geometry as SH and SV. A horizontal vibration oriented perpendicular to the in-line direction (particle motion purely horizontal) generates an SH-wave. If the horizontal vibration is oriented parallel to the in-line direction, the source generates an SV-wave, in isotropic media.

Shear wave data processing requires the rotation of the data acquired from the field coordinates to the radial-transverse coordinate system. The radial component (R) contains predominantly SV and P-wave modes, while the transverse (T) data are predominantly SH. 3D/3C acquisition records data from different azimuths. The data at a specific receiver is a mix of SV, SH, (and P) waves on each horizontal component. The degree of "mixing" depends on the location (azimuth and offset) of the receiver from the source. Rotation based on source-receiver azimuth is necessary to obtain separation of SV and SH waves (Simmons, 1999).

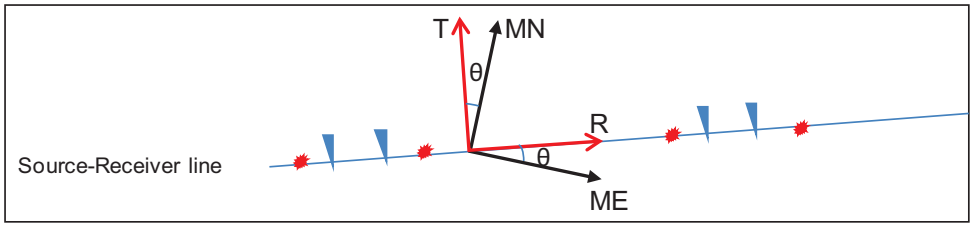

FIG. 1. Receiver orientation. MN is the magnetic north and ME is the Magnetic east (field orientation of the geophone components). R is the radial orientation and T is the transverse orientation (after rotation of geophone components).

The equation used for this rotation (Figure 1) was:

$$R = H_2 * \cos\theta + H_1 * \sin\theta \quad (1)$$

$$T = H_1 * \cos\theta - H_2 * \sin\theta \quad (2)$$

Where

R = Radial component

T = Transverse component

H_1= Data recorded on the magnetic North component (MN)

H_2= Data recorded on the magnetic east component (ME)

θ = Rotation angle

Plus-Minus time analysis method

The plus-minus time analysis method (Hagedoorn, 1959 and Dufour, 1996) is useful for both, depth and velocity determination. The basis of the plus-minus time analysis method lies in the traveltime reciprocity: The traveltime from source to receiver is the same as from receiver to source if they are interchanged. The basic geometry for this method is presented in figure 2.

The plus-times are used to give the traveltime from the surface to the refractor while the refractor velocity is estimated from the minus times. The plus-time (T^+_D) is defined as the sum of the traveltimes from two sources located on either side of a receiver minus the reciprocal time from shot to shot. The minus-time (T^-_D) is calculated by subtracting the times from the two sources located on either side of a receiver minus the reciprocal time.

To use this method, enough spread should be recorded in both directions, at least covering the whole distance between the sources. A window of analysis is defined between the two crossover points (from the forward and reverse curves, X_f and X_r, respectively). Inside this window, the plus-time value at each receiver can be evaluated with the following expression (see figure 2):

$$T^+_D = T_{AD} + T_{HD} - T_{AH} \quad (3)$$

From figure 2 and some simple mathematical manipulation, the expression for depth (at a specific receiver) for a two layer case can be defined as

$$h_1 = [(T^+_D)*(V_1)]/ (2*\cos(\theta c)) \quad (4)$$

The velocity of the first layer (V_1) can be found using the inverse slope for the best fit line of the first layer first break arrivals (source to crossover point). The second layer velocity (V_2) can be derived using the minus-time analysis over a window that includes only the second layer first break arrivals. θc is the critical angle, $\theta c = \sin^{-1}(V_1 / V_2)$.

For 3-layer case (Figure 3):

$$T_{AB'EFC'D} = 2*T_{AB'} + T_{EF} + 2*T_{B'E}$$

$$T_{AB'EFC'D} = \frac{2*h_1}{V_1*\cos\theta_{13}} + \frac{X_r - 2*h_1*\tan\theta_{13} - 2*h_2*\tan\theta_{23}}{V_3} + \frac{2*h_2}{V_2*\cos\theta_{23}}$$

$$T_{AB'EFC'D} = \frac{X_r}{V_3} + 2*h_1\left(\frac{1}{V_1*\cos\theta_{13}} - \frac{\tan\theta_{13}}{V_3}\right) + 2*h_2\left(\frac{1}{V_2*\cos\theta_{23}} - \frac{\tan\theta_{23}}{V_3}\right)$$

By Snell's Law

$\sin\theta_{13} = V_1/V_3$ and $\sin\theta_{23} = V_2/V_3$

$$T_{AB'EFC'D} = \frac{X_r}{V_3} + 2*h_1\left(\frac{1}{V_1*\cos\theta_{13}} - \frac{\sin\theta_{13}*\sin\theta_{13}}{\cos\theta_{13}*V_1}\right) + 2*h_2\left(\frac{1}{V_2*\cos\theta_{23}} - \frac{\sin\theta_{23}*\sin\theta_{23}}{\cos\theta_{23}*V_2}\right)$$

$$T_{AB'EFC'D} = \frac{X_r}{V_3} + \frac{2*h_1*\cos\theta_{13}}{V_1} + \frac{2*h_2*\cos\theta_{23}}{V_2}$$

From this equation the plus times can be defined as

$$T^+ = \frac{2*h_1*\cos\theta_{13}}{V_1} + \frac{2*h_2*\cos\theta_{23}}{V_2}$$

After some manipulation, the depth of the second layer can be obtained.

$$h_2 = \left[T^+ - \frac{2*h_1*\cos\theta_{13}}{V_1}\right]*\frac{V_2}{2\cos\theta_{23}} \qquad (5)$$

V_3 can be obtained from the ΔT^-_D vs. ΔX curve for the appropriate window.

θ_{23} is the critical angle, calculated following Snell's law as $\sin^{-1}(V_2/V_3)$

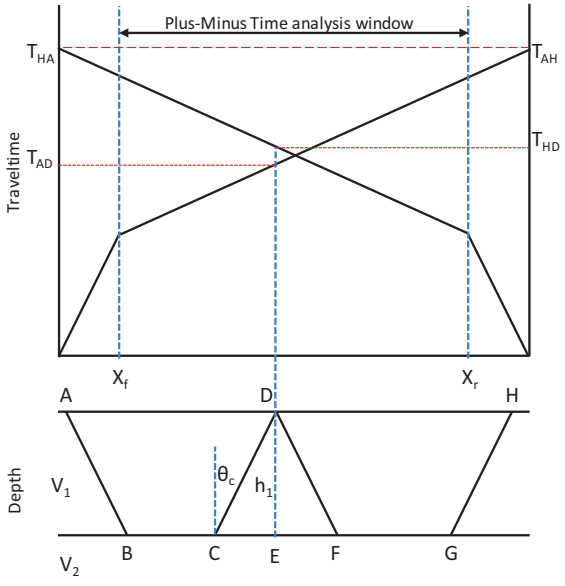

FIG. 2. Plus time analysis according to the plus-minus method of Hagedoorn (1959)

The minus-time at a receiver D (Figure 4) is

$$T^-_D = T_{AD} - T_{HD} - T_{AH} \qquad (6a)$$

The minus-time at a receiver D' is

$$T^-_{D'} = T_{AD'} - T_{HD'} - T_{AH} \qquad (6b)$$

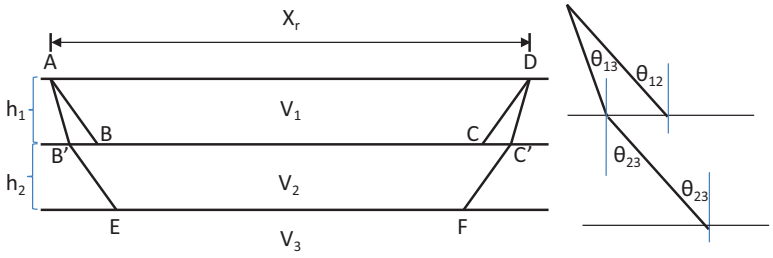

FIG. 3. Source (A) to receiver (D) path for three layers separated by horizontal interfaces

Subtract 6a from 6b

$$T^{-}_{D'} - T^{-}_{D} = T_{AD'} - T_{HD'} - T_{AH} - T_{AD} + T_{HD} + T_{AH}$$

$$T^{-}_{D'} - T^{-}_{D} = T_{AD'} - T_{AD} + T_{HD} - T_{HD'}$$

$$T^{-}_{D'} - T^{-}_{D} = \Delta X/ V_2 + \Delta X/ V_2$$

$$T^{-}_{D'} - T^{-}_{D} = 2*\Delta X/ V_2 \qquad (7)$$

Where, T is the time from shot (A, H) to receiver (D, D'). ΔX is distance between consecutive receivers. The velocity of the second layer (V_2) is equal to twice the inverse slope of a best fit line through the difference in minus-time ($T^{-}_{D'} - T^{-}_{D}$) calculated inside the plus-minus time analysis window.

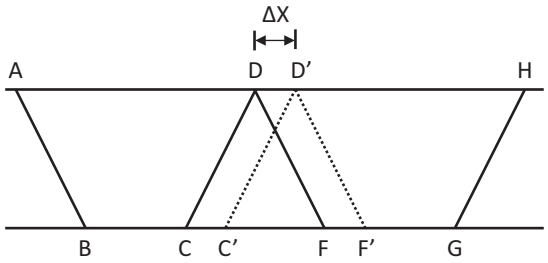

FIG 4. Raypaths for a reversed refraction profile to illustrate the Hagedoorn or plus-minus method

Summary of the method

Knowing the first and second layer velocities and the plus-time values at each receiver, the thickness of the first layer below each receiver can be found according to the delay time analysis. The delay time represents the time to travel from the receiver to the refractor minus the time necessary to travel the normal projection of the raypath on the refractor (Figure 2). From Snell's law, a relation between the delay times (left and right) and the thickness of the first layer at the receiver can be established. Finally, the link between the delay times and the plus-times allows us to determine the thickness of the first layer below each receiver inside the plus-minus time analysis window (equation 4). This will allow the determination of the first layer thickness all along a seismic survey line, from which surface-consistent static corrections are extracted. This analysis is for a two layer case in two dimensions.

Study area and geology

The Devonian Horn River Basin shales were deposited in deep waters at the foot of the Slave Point carbonate platform in northeast B.C (Figure 5). These shale units are widespread in northeast Brithish Columbia (NEBC), covering approximately 80000 km^2. Organic rich units within the Exshaw, Muskwa and Evie formations are the main targets in the area.

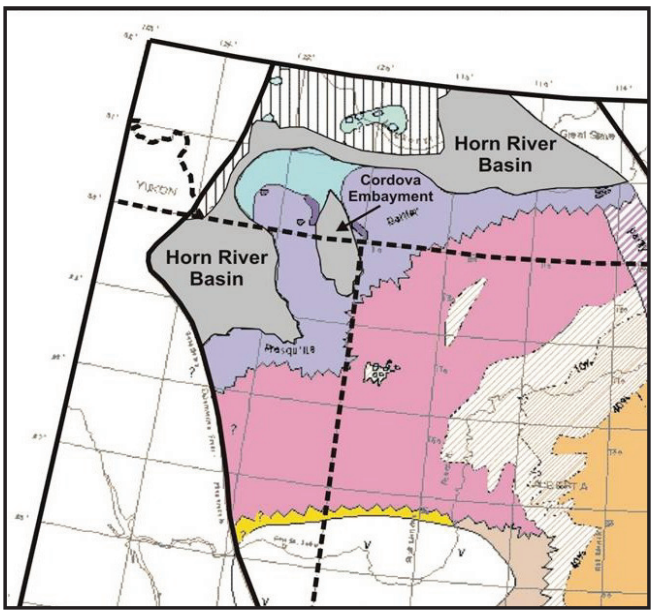

FIG. 5. Location Map: Northeast British Columbia

Stratigraphy and depositional history

Lower Keg River formation (Keg River Formation): It is uniform in general across much of NEBC with thickness ranging from 20 to 50 m. North of Clarke Lake, Evie shales join the upper part of the Keg River Platform. To the south, carbonates are gradually replaced by clastic deposits. The Lower Keg River marks the beginning of a widespread marine transgression with relatively deep-water deposits (Figure 6).

Upper Keg River Formation: This carbonate strata forms the northern wall of the Elk Point restricted basin, with thickness greater that 200 m. This formation consists of stacked cycles, each with a shaly base, shoaling upwards to a thick high energy carbonate at top.

Sulphur Point Formation: These carbonates were deposited during a relatively subtle regional transgression over the Keg River. In the south, the basal contact is sharp, as relatively high energy peloidal grainstone-wackestone transgress the evaporitic Muskeg.

Slave Point Formation: It was deposited in the early stages of a basin-wide transgression. It forms a thick and complex carbonate platform including several stacked shallowing-upward cycles. Reefal buildups and high energy carbonate banks occur along the edges of the main platform and also along the margins of platform-interior embayments.

Evie, Muskwa, Otter Park formations: Middle Devonian shales forming the Horn River Group (Morrow, 2002). The Evie/Klua shale is correlated with Elk Point (Keg River and Sulphur Point) carbonates. Dark, radioactive Evie shales represent a starved basin facies, deposited when Keg River buildups restricted water circulation and cut off the interior evaporitic (Muskeg) platform. The Otter Park includes shales that filled Slave Point embayment and capped the Slave Point Platform. The Muskwa is assigned to the Upper Devonian Woodbend Group, where it represents the distal starved basin component of the Fort Simpson basin-filling shales.

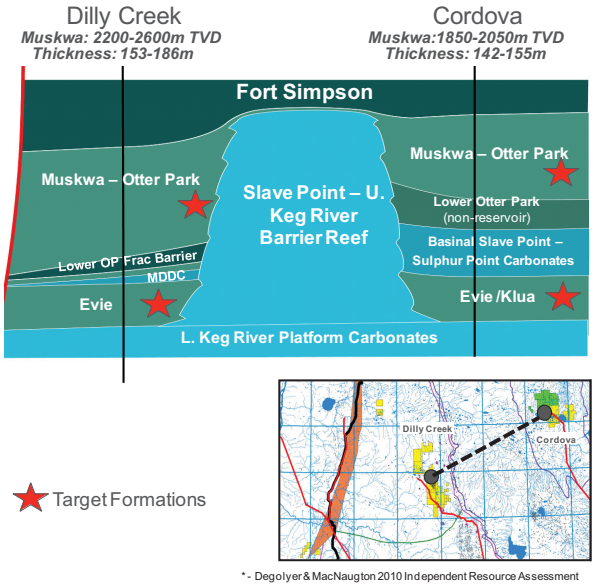

FIG. 6. Stratigraphy of the study area

Velocity and depth analysis

The procedure to find velocity and depth for the shallow layers was applied to both compressional and shear datasets.

The first step was to analyse the data and to determine the orientation of the receivers and the source as this information was not clear from the acquisition reports. The H_1 component of the geophone was oriented zero degrees (magnetic). The azimuth of the line was 88° and the magnetic declination in the area is 20°. The rotation angle is the angle between the transverse (T) component and the magnetic North, 22° in this case (Figure 1). Equations 1 and 2 were used to rotate the data.

As the source was vibrating perpendicular to the line direction, the maximum energy was obtained in the transverse component, i.e. SH-SH by convention.

Examples of shot gathers before and after rotation are shown in figure 7. Note how the transverse component has more energy than the radial component as expected. This is due to coupling between the crossline vibrations and the transverse geophone component.

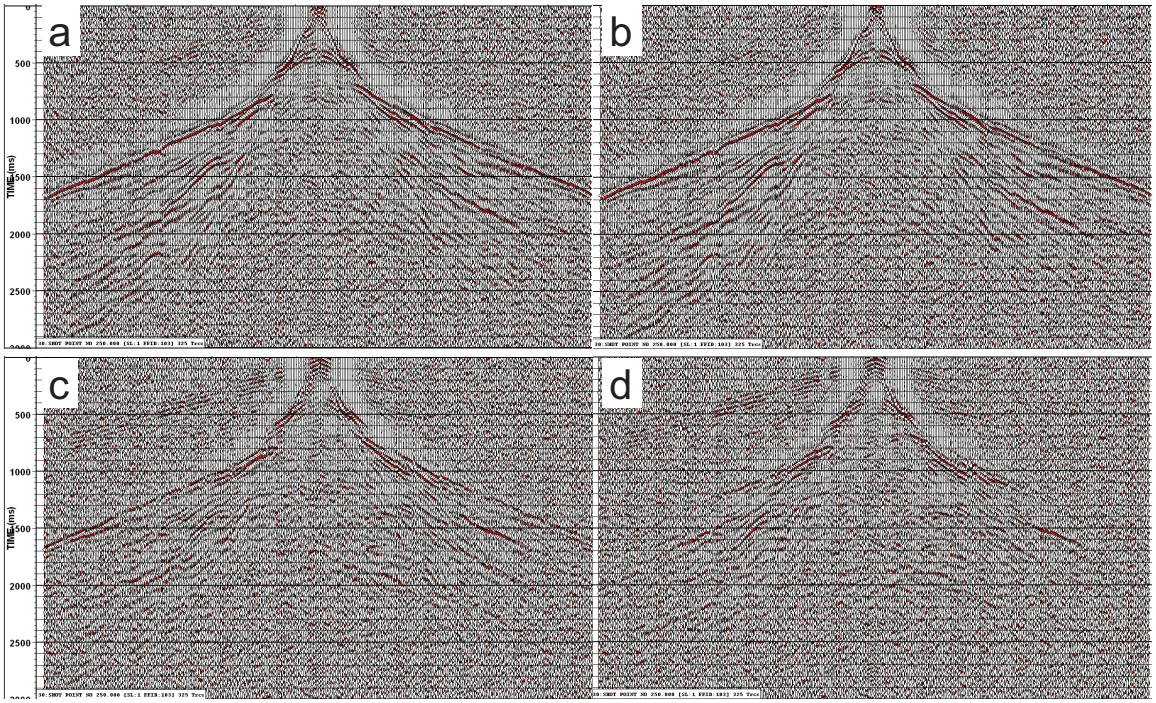

FIG. 7. a) SH-H1 data, b) SH-T data, c) SH-H2 data, d) SH-R data. AGC with 500 ms window and filter 5-10-25-30 applied.

The second step in the process was to pick first breaks for both datasets, SH-T data and P-V data. Example of these first break picks is shown in figure 8. From here onwards in this report, P-V refers to P-wave data and SH-T refers to shear-wave data or SH data.

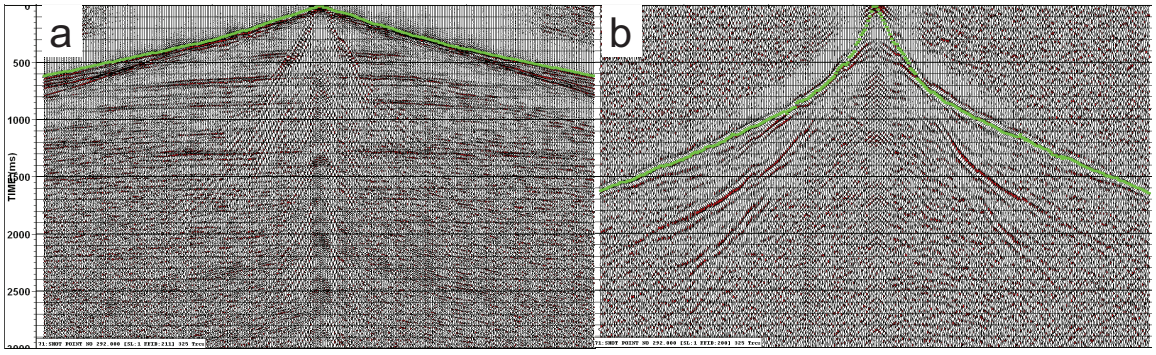

FIG. 8. First break picks for P-V data (a) and SH-T data (b). AGC with 500 ms window and filters applied.

Analysing curves of SH-T first break times versus location (or offset), three layers were detected to the west end and two layers to the east (Figure 9) of the line. From the P-V data only two layers were detected for the entire section (Figure 10). V_i (i= 1, 2, or 3) indicates the velocity for first, second and third layer, respectively.

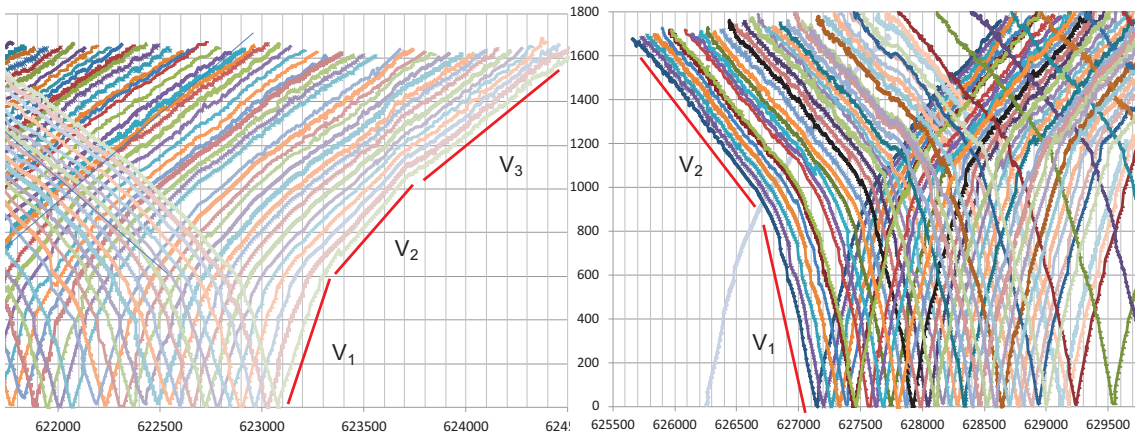

FIG. 9. SH-T first break times versus receiver location. Threes layers detected in the west end of the line (left), two layers detected in the east end of the line (right)

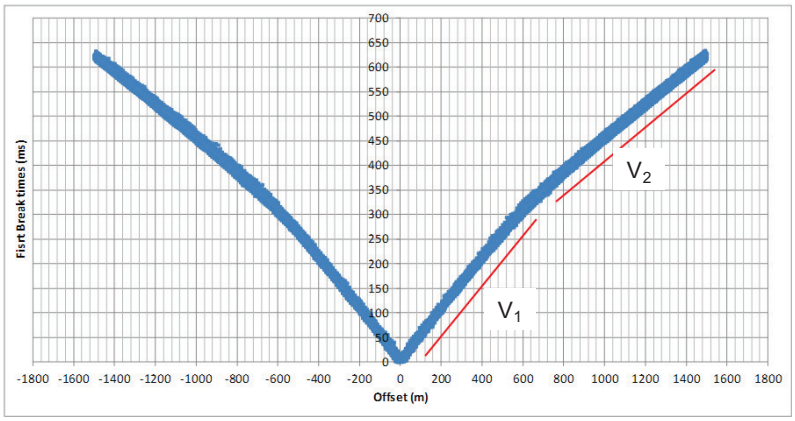

FIG. 10. All P-V first break times versus offset.

SH-T data analysis

The plus-minus time analysis was used to obtain the velocities and depths. For the shear data this process was carried out manually, and also through a program code in order to validate results. The manual process used Excel spreadsheets to apply the method; plus and minus times were calculated using equations 3 and 6. V_1 was calculated directly from the first breaks of the first layer and V_2 was obtained through curves of T^- vs. distance (Figure 11). This method requires pair of shots to make the analysis and the definition of the analysis window between the crossover points (every 10^{th} or 20^{th} shot); these shots were chosen so that the entire profile is covered at least once. There is no redundancy of depth or velocity results for each receiver.

Depths were calculated using equations 4 or 5 depending on the case, two or three layers. The results for velocities and depths are shown in figures 12 and 13.

As previously mentioned, three layers were detected from the first break times from the west end of the line. Around shot 310 (stn 1367) the second layer was decreasing in thickness so the analysis window, which is determined between the crossover points, was

too small and this prevented the second shot be located inside the refractor being analysed. Consequently the second refractor was not clearly identified in this section. To the east of station 1600 only two layers were considered (one refractor).

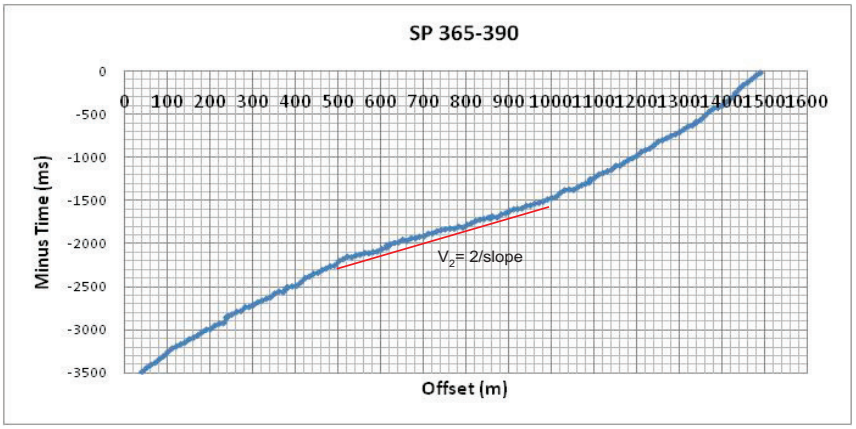

FIG. 11. Example of T^- vs. offset curve generated for to find V_2 with the minus times

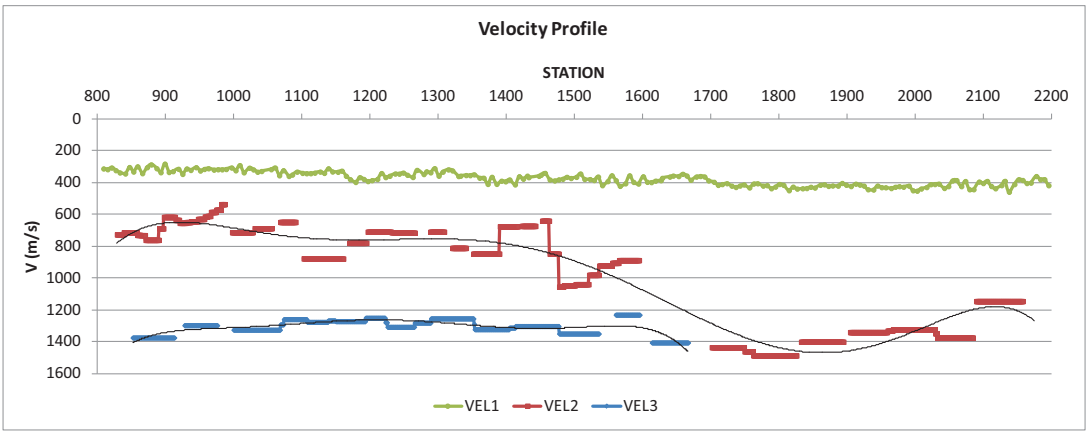

FIG. 12. Velocity profiles obtained by manually applying the plus-minus time analysis method on SH-T data

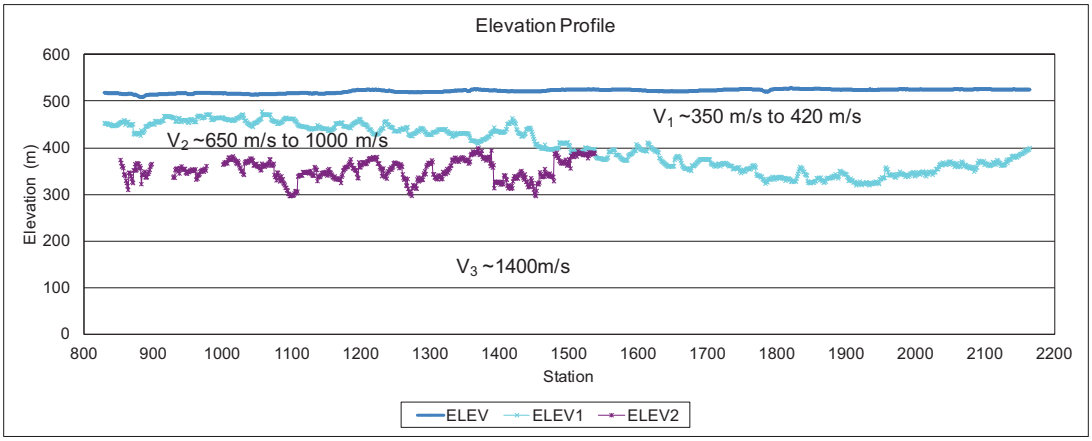

FIG. 13. Elevation profile obtained by manually applying the plus-minus time analysis method on SH-T data

The plus-minus time analysis was also applied through a program code that requires the first break picks as an input and it will generate velocities for the entire profile. Other input parameters for this program are the minimum window offset, minimum shot to shot offset (stations) and maximum shot to shot offset (stations). These values specify the analysis window for each pair of shots. Every shot is used with a combination of shots from the segment between the minimum shot to shot offset and maximum shot to shot offset. The minimum window offset identifies the lower limit of the window for plus and minus times calculations. The minimum shot to shot distance should be at least twice the minimum offset window (Figure 14).

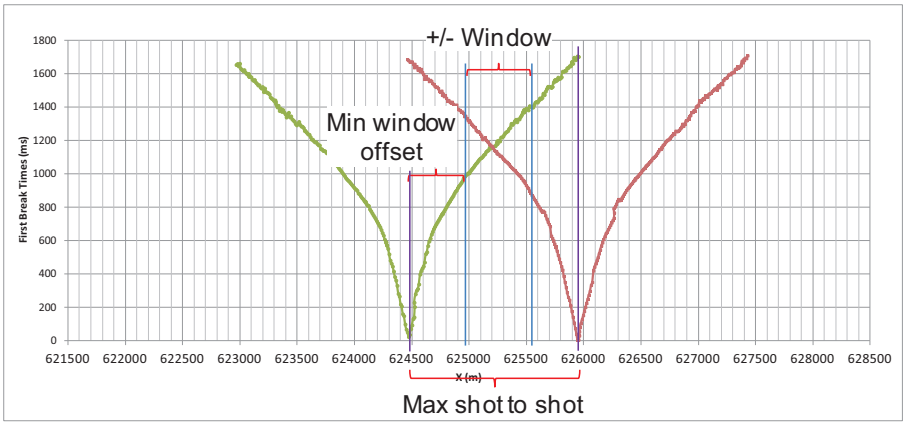

FIG. 14. Input parameters for the program code

The velocities obtained with this program are shown in figure 15. Figure 15a shows the raw results from the program, figure 15b shows the velocity profile smoothed through a polynomial function of grade 10 generated with Matlab. Figure 15c is a final composite of velocities for the profile. From figures 15a and 15b, it can be seen that V_1 and V_2 tend to the same value east of station 1500, suggesting that a layer is disappearing in the area marked as transition zone (Figure 15b). This was confirmed by the manual calculation where from shot 310 (stn 1367) to shot 355 (stn 1659) it was not possible to apply the plus-minus time analysis due to insufficient sampling of the second layer (the thickness was decreasing);

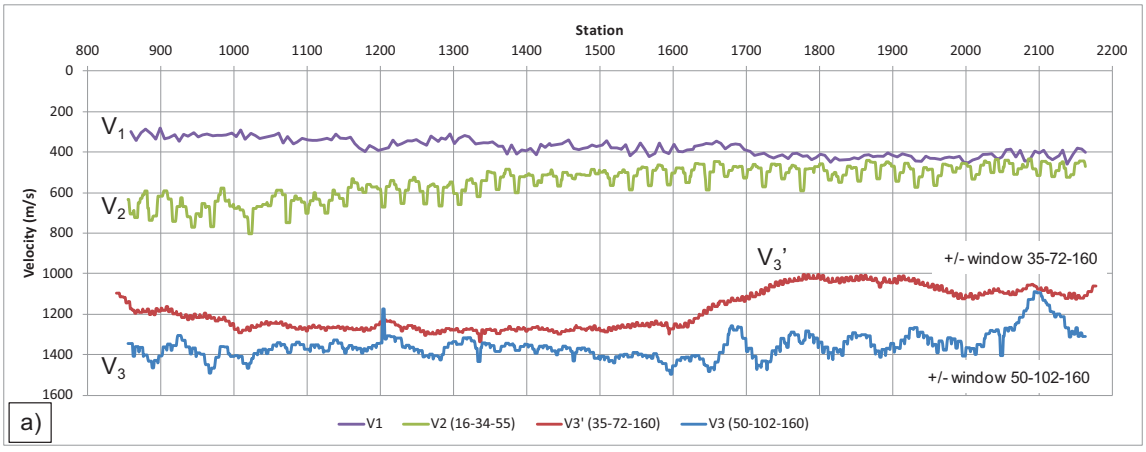

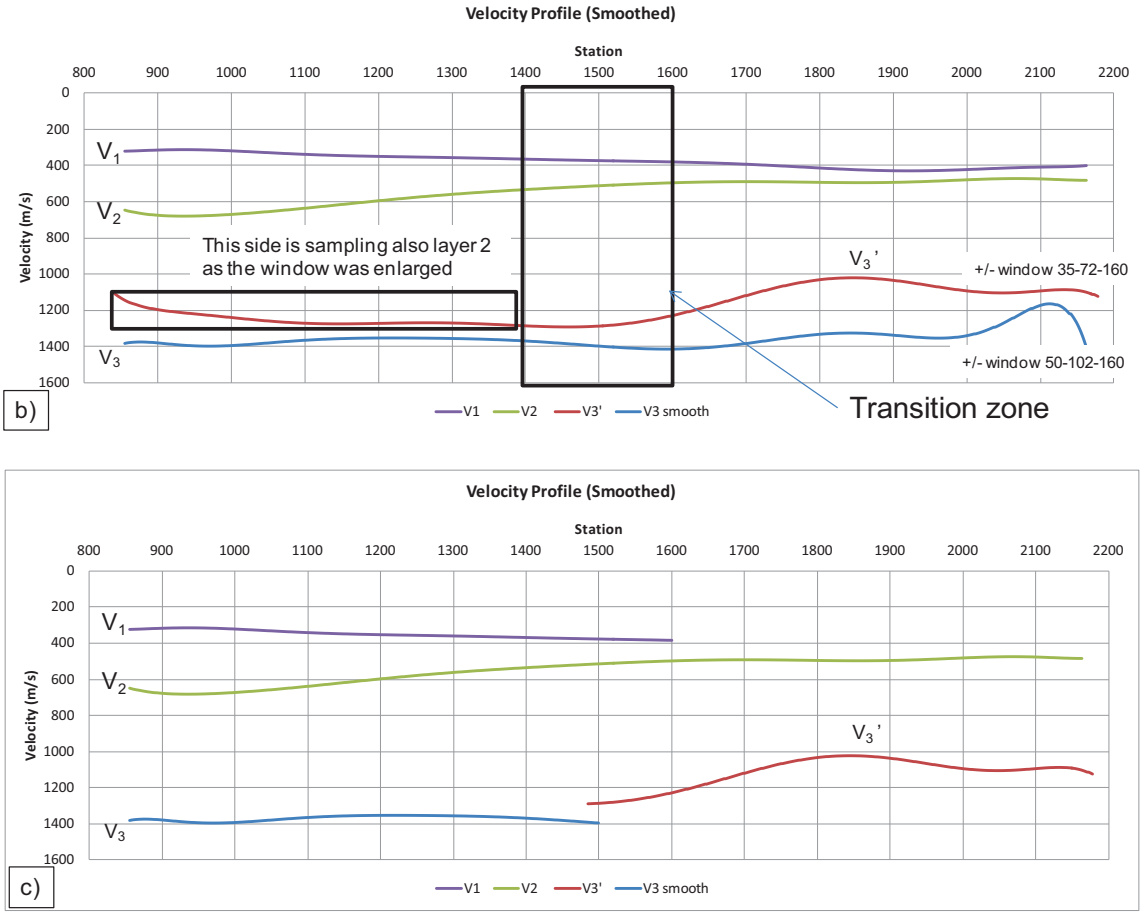

FIG. 15. Velocities obtained with the program code for the SH data. a) Raw velocities, b) Smoothed velocities, c) final velocities

For the deeper refractor, the velocity was the result of two different analysis widows. The red curve (V_3') was the result of a wider window to sample the deeper layer, but as there is a second layer to the west, this window was also sampling this layer in that side causing the decrease in velocity (see note in figure 15b). This figure shows the results with the optimum window found after several attempts. The velocity in the first layer ranges from 350 m/s to 420 m/s, for the second layer it goes from 500 m/s to 680 m/s and for the third layer there is a lateral variation from 1400 m/s to the west to 1100 m/s to the east.

The depth profile obtained using the velocities of figure 15c, is shown in figure 16. It was difficult to define the refractor boundaries between station 1400 and 1600. Here the assumption was that layer 2 is thinning. This depth profile is also confirming the presence of a channel in the area that has been previously detected with an electromagnetic survey (EM acquired by Nexen). The lower velocity to the east does not reflect the deeper refractor but a mix of materials due to the presence of the channel.

There is good agreement between the model generated manually and the model generated with the program code. The benefit of the last one is that the results are generated faster; the benefit of doing the process manually is that changes in velocity or

depth (changes in the near-surface) can be detected as the pairs of shots are analysed along the line.

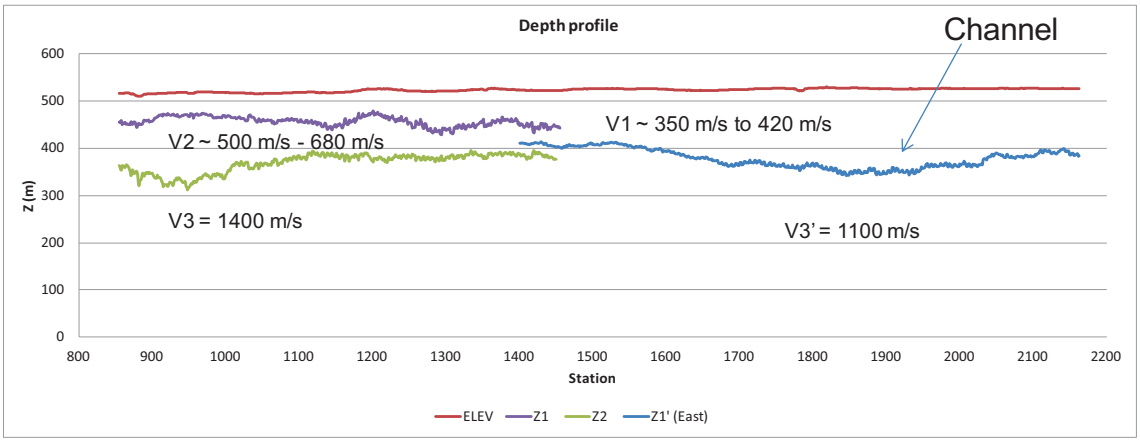

FIG. 16. Depth profile obtained from SH-wave data

P-wave data analysis

For the P-wave data, the plus-minus time analysis was only performed manually as the lack of longer offsets made difficult to determine the plus-minus windows. The analysis had to be more detailed to choose the correct pair of shots in order to perform the computations. The minus times were used to calculate the velocities (Figure 17) and the plus times to convert to depth (Figure 18) where the channel can be seen to the east end. The analysis of the first break times against offset showed the presence of two layers (Figure 8).

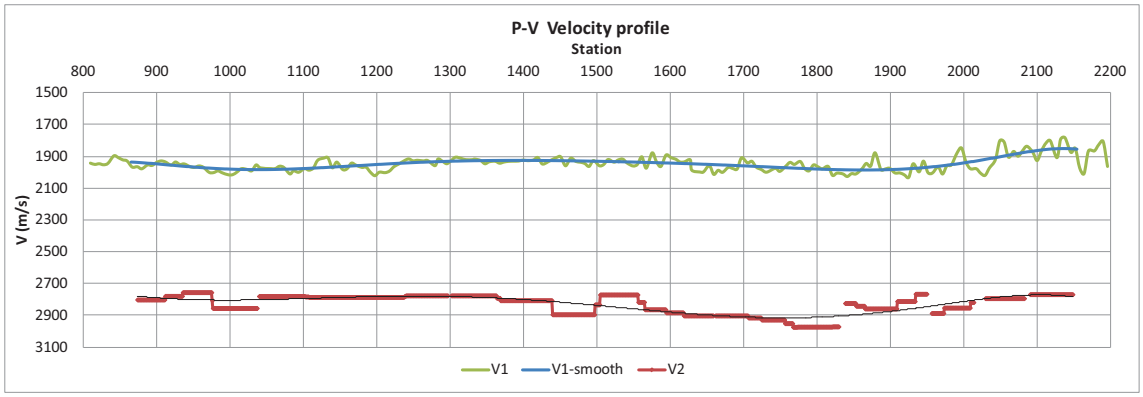

FIG. 17. P-wave velocity profile for layer 1 (V_1) and layer two (V_2)

The average velocity for the first layer is 1950 m/s and for the second layer is 2800 m/s. The velocities shown in figure 17 were used to calculate depth for a two layer case (equation 4). The depth profile is shown in figure 18, where a subtle channel can be seen starting from station 1600 to station 1950.

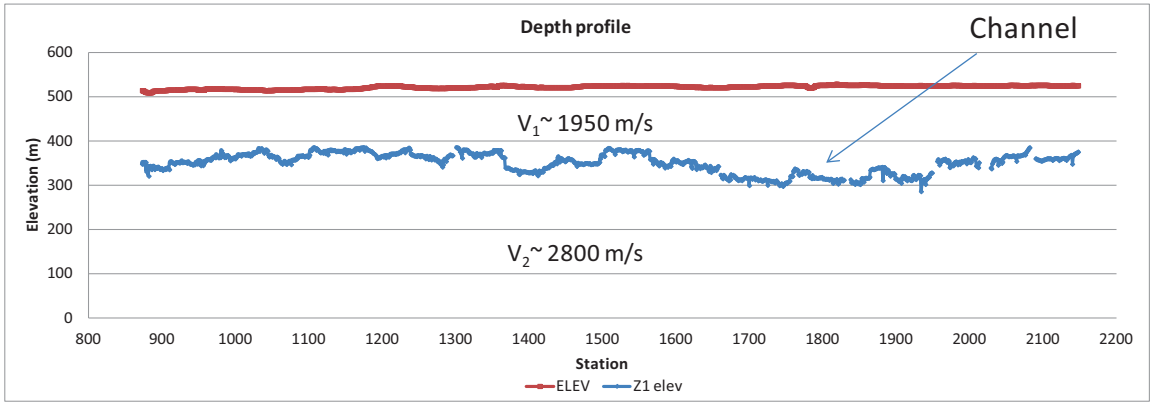

FIG. 18. Depth profile obtained from P-wave data

A comparison with the generalized linear inversion (GLI) method was made (courtesy of Sensor Geophysical). In this method a three layer model was assumed for both P-V data and SH data (Figure 19). For the P-V data, a velocity of 1000 m/s was assumed for the first layer; an average of 1950 m/s for the second layer and an average of 2900 m/s for the third layer were obtained. The depth for the first layer varies from 1 m to 10 m and for the second varies from 140 m to 210 m. For the SH data, a velocity of 350 m/s was assumed for the first layer, 500 to 900 m/s for the second and an average of 1400 m/s for the third layer were obtained. The depth for the first layer varies from 50 m to 90 m and for the second varies from 180 m to 210 m.

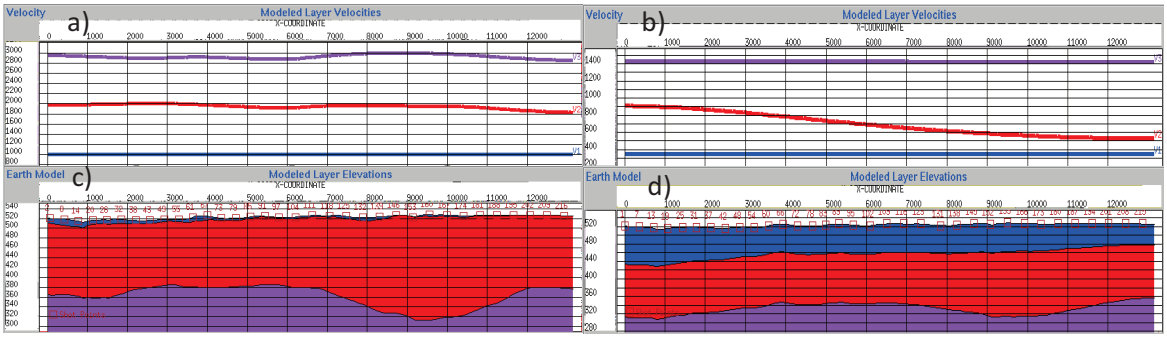

FIG. 19. Results from the GLI method. a) P-wave velocity profile, b) SH-wave velocity profile, c) P-wave depth profile, d) SH-wave depth profile

Comparing this figure with the results from the plus-minus analysis method, it is noticed that they have good agreement in terms of velocities. However, the depth profile shows some differences. The depth of the deeper refractor is similar in both methods but there are some differences in the general model. The P-wave data assumed 3 layers but the first layer is very thin and disappears to the east end on the line; this is close to the plus-minus method where only two layers were considered. For the SH model, three layers were interpreted for the GLI method, the deeper refractor is similar in both methods; the difference is that for the GLI method, the three layers are present for the entire profile while for the plus-minus method, there are three layers to the west and only two layers to the east. The GLI method forces three layers along the profile while the plus-minus

method gives the flexibility to choose different analysis windows depending on what the data shows.

Statics correction calculations

The best definition for static corrections is given by Sheriff (Sheriff, 1991): "Correction applied to seismic data to compensate for the effects of variations in elevations, weathering thickness, weathering velocity, or reference to a datum. The objective is to determine the reflection arrival times which would have been observed if all measurements had been made on a (usually) flat plane with no weathering or low-velocity material present. These corrections are based on uphole data, refraction first-breaks and or event smoothing".

This definition was applied to the P-V and SH models shown in figures 16 and 18. Based on Sheriff's definition, time corrections must be applied to data recorded at all surface locations to convert them to a set of times that would have been observed had the data been recorded on the datum surface with no weathering or low-velocity material present below this plane.

The first step is to remove the weathering layer (or low-velocity layer, LVL) so that the base of this layer becomes the new reference surface. The times are corrected as if they have been observed on this new reference. This correction is often called the weathering correction, T_w. The second step is to adjust the data to simulate data recorded at another reference surface called the datum. This correction is often called the elevation correction, T_e (Cox, 1999). The datum correction (T_d) must include both the weathering correction and the elevation correction to remove the time effect of the weathered layer and to adjust the times to a datum elevation.

$$T_d = - Tw \pm Te \tag{8}$$

There is an intermediate correction to the surface (T_g) which is defined as

$$T_g = \left(-\frac{H_1}{V_1} - \frac{H_2}{V_2} \right) + \left(\frac{H_1 + H_2}{V_3} \right) \tag{9}$$

The datum correction (T_d) is defined as

$$T_d = -\frac{H_1}{V_1} - \frac{H_2}{V_2} + \left(\frac{\left(E_d - E_g\right) + H_1 + H_2}{V_3} \right) \tag{10}$$

H_1 and H_2 are the thickness of layers 1 and 2, respectively. V_1, V_2 and V_3 are the velocities of layer 1, 2 and 3, respectively. E_d is the datum elevation and E_g is the surface elevation where the geophones are located (Figure 20).

In general, a negative static correction reduces the reflection time. If the datum is located above the surface, then the elevation correction has a positive sign. The weathering correction will always be negative.

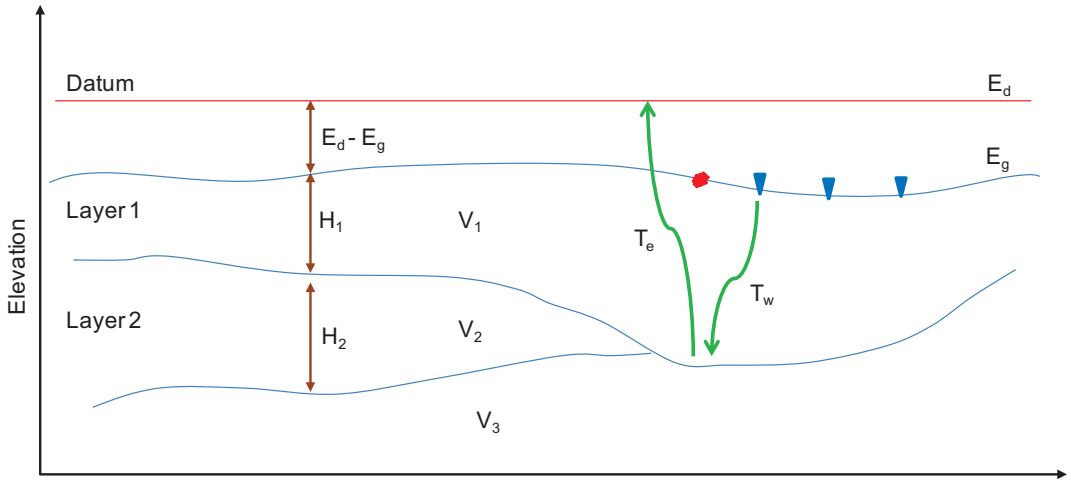

FIG. 20. Schematic diagram illustrating components of datum static corrections

Figure 21 shows the receiver datum static corrections for the SH wave data. The blue curve represents the result for a three layer case (model to the west) and the red curve is the result for a two layer case (model to the east). Higher static corrections are needed to the east due to a thicker layer 1 with lower velocity. The elevation in the area ranges from 515 m to 526 m and the datum was located at 550 m. Figure 22 show the receiver static corrections for the P-V data. They also reflect the need of higher correction to the east end similar to the SH statics.

As a consequence of the low SH velocities, the magnitude of SH datum static corrections is typically many times greater than for the corresponding P-V values. Figures 21 and 22 show a profile with datum static corrections of -160 ms to -330 ms for SH data and about -10 ms to -28 ms for P-V data. Shear wave statics are usually ten times or greater than the P-wave static. This relationship is also reflected in the velocity ratio between compressional and shear data for the shallow layers (Figure 23). For this reason, S-wave statics are difficult to estimate with confidence. (Tatham, 1991).

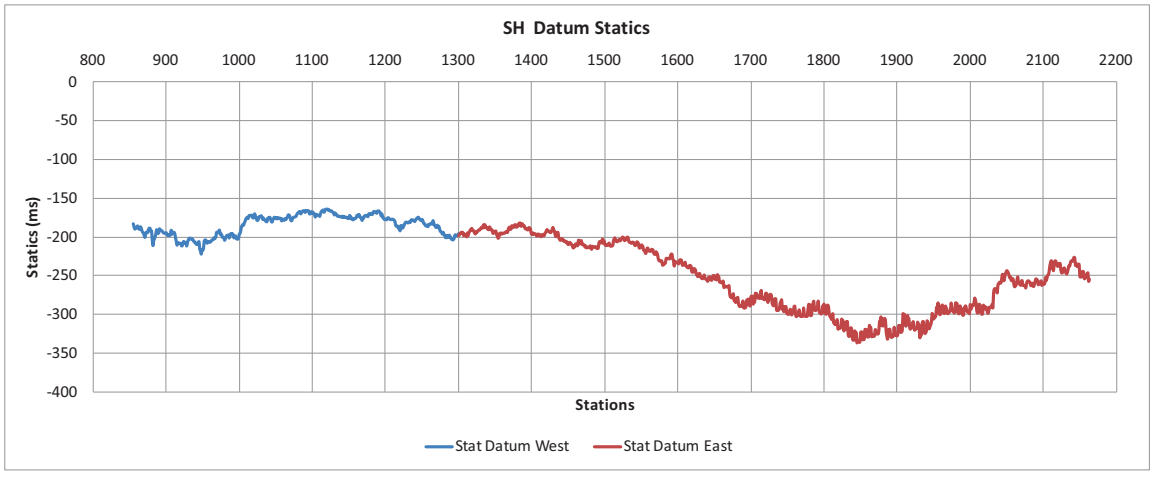

FIG. 21. Receiver static corrections for SH-wave data.

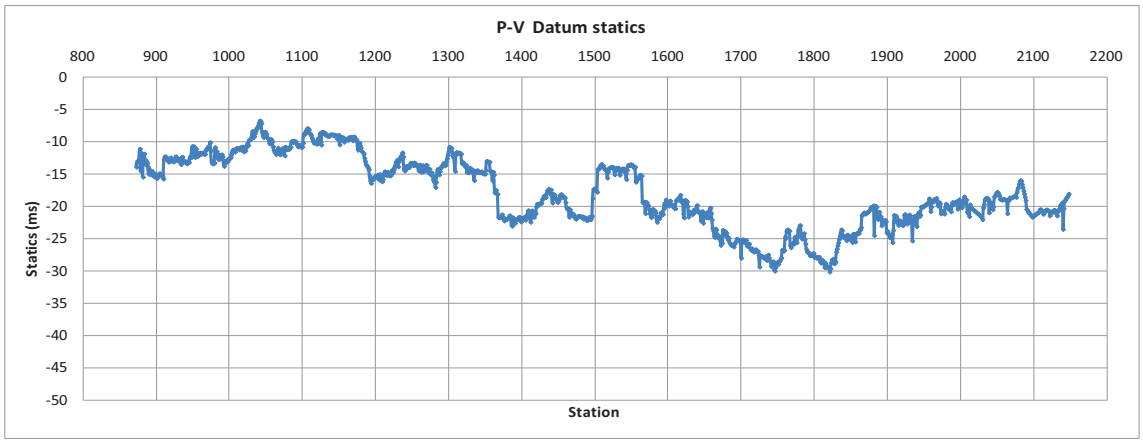

FIG. 22. Receiver static corrections for P-wave data.

The static corrections times are negatively higher around the channel due to the lower velocity and thicker layer in this area. This lower velocity produces increased time for reflections coming from deeper events. That is the reason of high negative values in static that will shift the data up.

The Vp/Vs ratio can be appreciated in figure 23. It can be noticed the high Vp/Vs values for the first layer, reaching values up to 6. For shallow layers, values of 3 to 4 are expected. This relationship is due to high P velocity relative to the low SH velocity in the area. The deep Vp/Vs ratio reflects the usual value expected for this relationship, between 2 and 3.

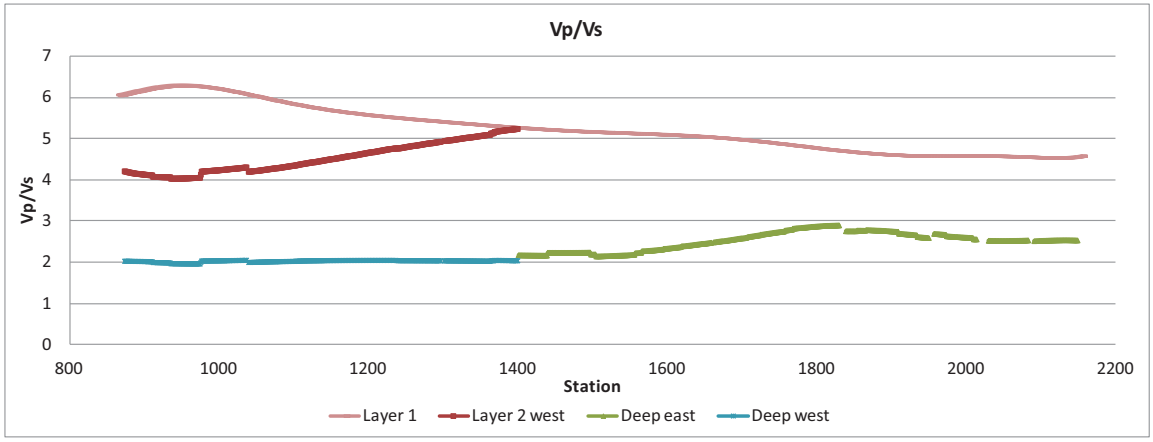

FIG 23. Vp/Vs along the profile

PP and PS well logs

Very important information available is a well log acquired in the survey area, with a complete set of curves taken over the entire length of the well, i.e. from 40 m to 2054 m. The compressional sonic log and the shear sonic log were used to calculate shear and compressional velocities (Figure 24) and from there, the Vp/Vs ratio (Figure 25). Note that the velocities in the shallow section (0-300 m) are comparable with the velocities obtained from the plus-minus method. S-wave velocity of 500 m/s from 40-170 m and an

average of 1200 m/s from 170-270 m; P-wave velocity of ~2000 m/s from 40-150 m, increasing from there to around 2800 m/s from 200-250 m depth. Synthetic seismograms (Figure 26) were generated with the software Syngram, and used to tie the seismic data (Figures 27, 28). P- and S-wave velocity ratios (Vp/Vs) can be calculated from the P-wave (PP) time and converted wave (PS) time extracted from the synthetic shot gathers (equation 11). This relationship can be used to register the PP and PS data.

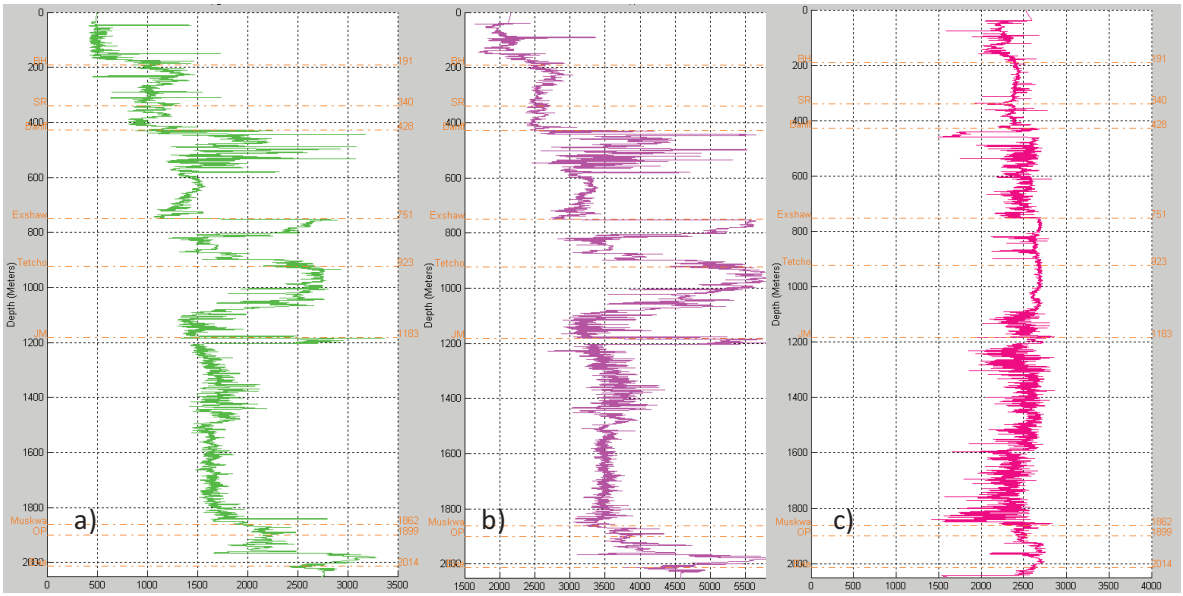

FIG. 24. Well log from the area. a) S-wave velocity log. b) P-wave velocity log. c) Density log

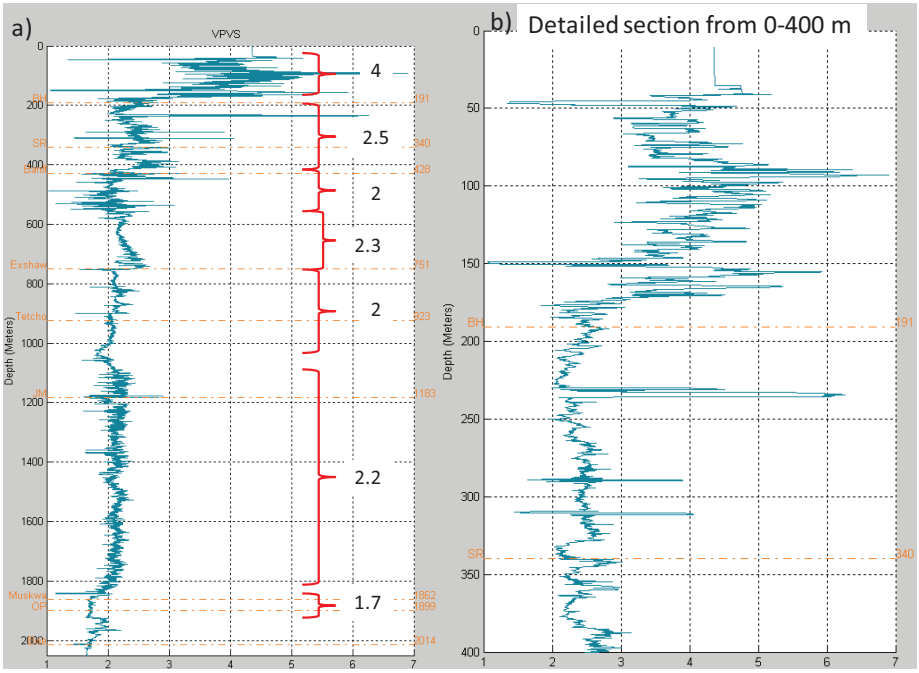

FIG. 25 Vp/Vs calculated from dipole sonic log. a) Complete length of the Vp/Vs log. b) Detailed view of the Vp/Vs log from 0-400m

$$V_P/V_S = (2*\Delta T_{PS} - \Delta T_{PP}) / \Delta T_{PP} \quad (11)$$

Where

ΔT_{PS} is the converted wave time difference between two consecutive interfaces

ΔT_{PP} is the P-wave time difference between two consecutive interfaces

The synthetic seismogram was generated with a Ricker wavelet of 40 Hz for the PP data and 20 Hz for the PS data. The time for the deepest reflection in the PP gather is around 1.2 seconds and in the PS gather is around 2.1 second. The relationship of times between the two datasets and the Vp/Vs ratio from the well logs are shown in table 1.

Figure 25 shows the Vp/Vs ratio obtained from the well sonic logs. Average values are shown on the right and are also presented on the right column in table 1.

Table 1. Vp/Vs ratio from the well log

Tops		Tp	Tps	ΔTpp	ΔTps	Vp/Vs
Bucking Horse	BH	0.17	0.42	0.17	0.42	4.0
Spirit River	SR	0.32	0.68	0.150	0.260	2.5
Banff	Banff	0.38	0.77	0.060	0.090	2.0
Exshaw	Exshaw	0.55	1.05	0.170	0.280	2.3
Jean Marie/ Fort Simpson	JM/FS	0.78	1.40	0.230	0.350	2.0
Muskwa/Otter Park	M/OP	1.13	1.96	0.350	0.560	2.2
Evie	Evie	1.20	2.05	0.070	0.090	1.7

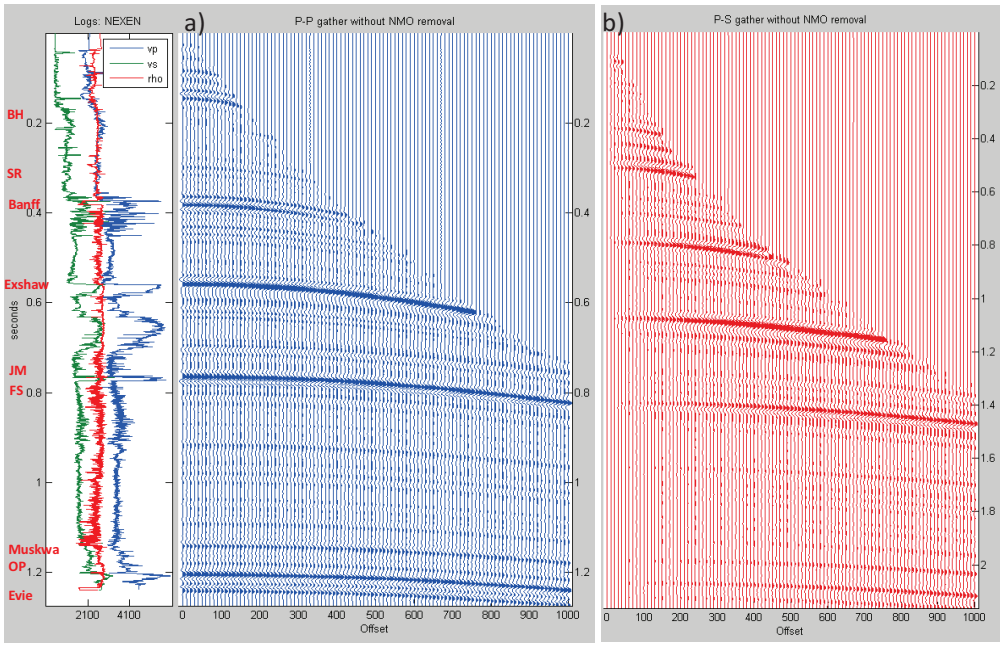

FIG. 26. Synthetic seismogram in time. a) PP gather and b) PS gather

It can be seen in figures 27 and 28, good agreement between the generated synthetic seismogram and the field seismic data. For the converted wave data, the time of the reflectors is different because the shot was chosen far from the well (~5 km away). The

shots close to the well log did not present good signal to noise ratio therefore the reflectors could not be identified. The agreement for the P-wave data is almost perfect, except for the shallow reflectors as they were contaminated with ground roll. An F-K filter was applied to attenuate this noise but still the shallow reflectors are not clear.

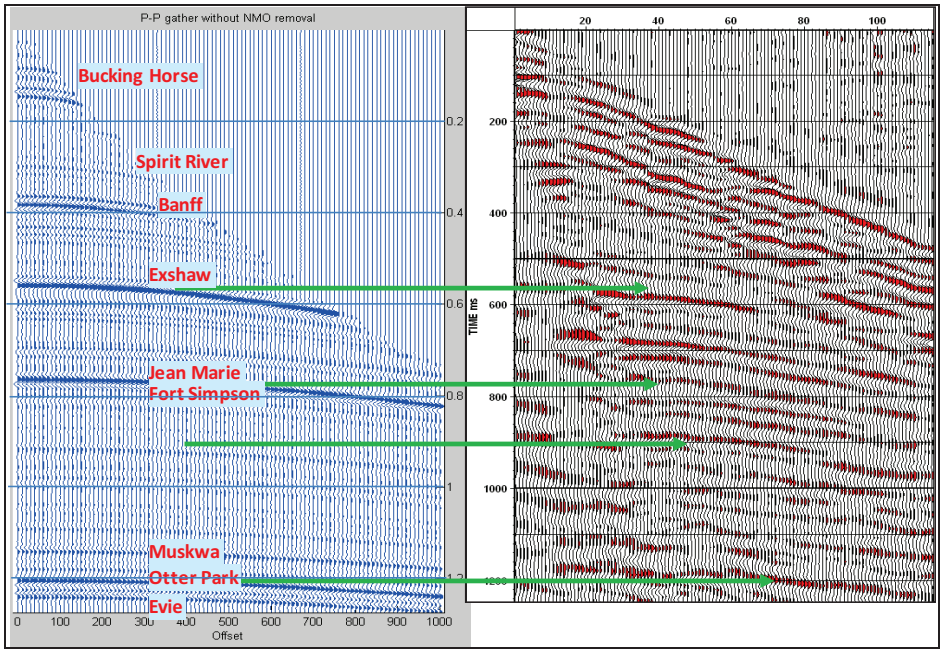

FIG. 27. Synthetic P-wave (PP) gather in time (left), field P-wave shot gather (right)

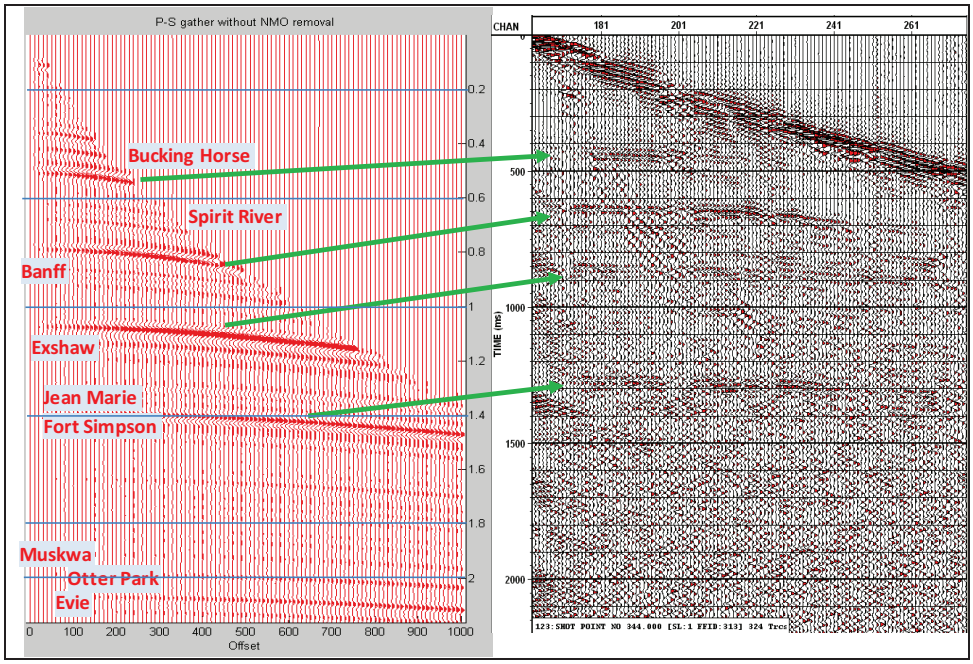

FIG. 28. Converted-wave (PS) gather in time (left), field PS-wave shot gather (right)

Sensor Geophysical carried out the processing of P-V data, SH data and converted wave data (PS). Registration of P-wave, SH-wave and PS data is presented in figure 29. The

function Vp/Vs used for this registration was 3.2 from 0-1050 ms, 2.3 from 1050-1380 ms and 2.0 from 1380 to the end of data time.

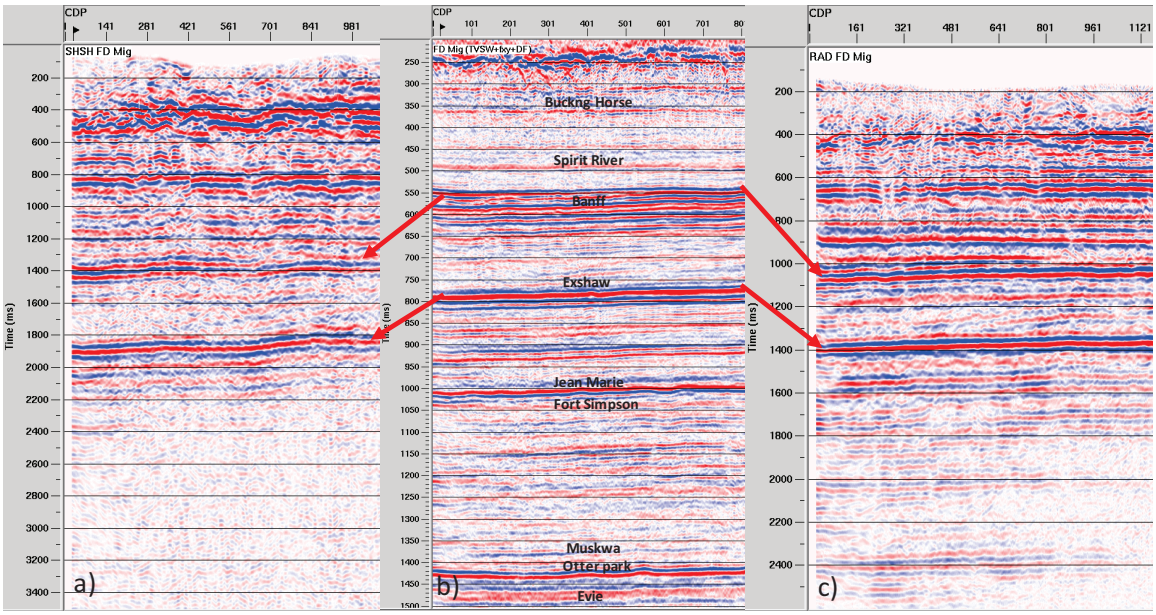

FIG. 29. a) migrated SH-wave section, b) migrated P-wave section and c) migrated PS section

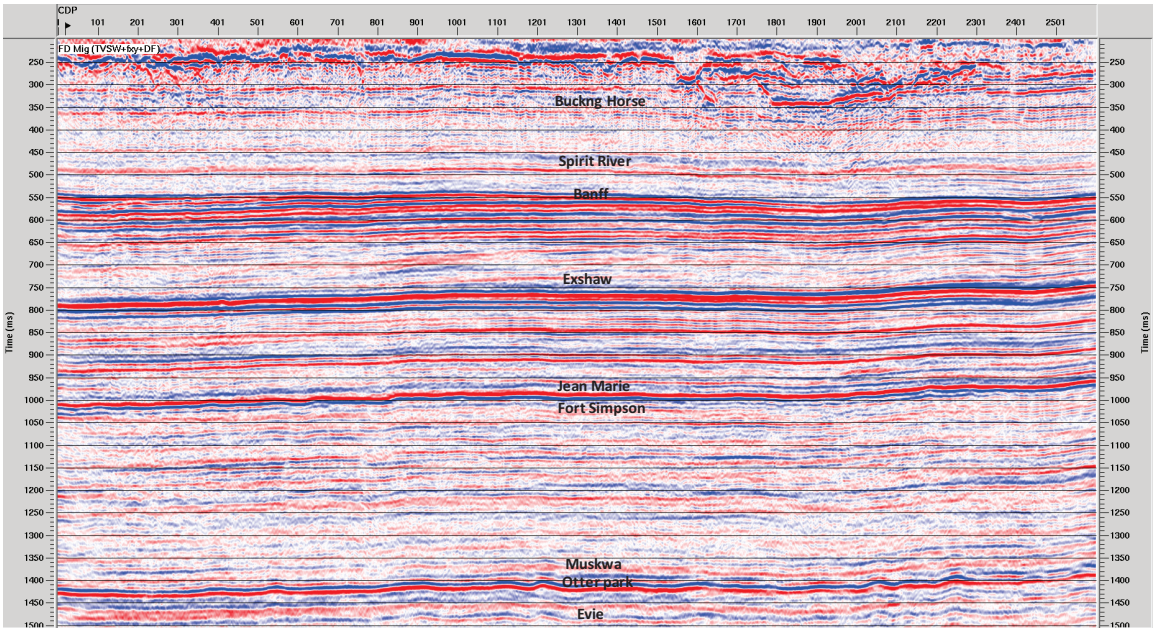

FIG. 30. P-wave section after post-stack migration

Figures 30, 31 and 32 show the sections obtained after processing the P-wave data, the SH data and the PS data. The channel that was detected with the refraction method applied can be seen from CDP ~1800 to CDP ~2100. The main units in the area are also included in these figures. SH and PS sections show appreciably good results with reflections up to 2 seconds and 2.4 seconds, respectively.

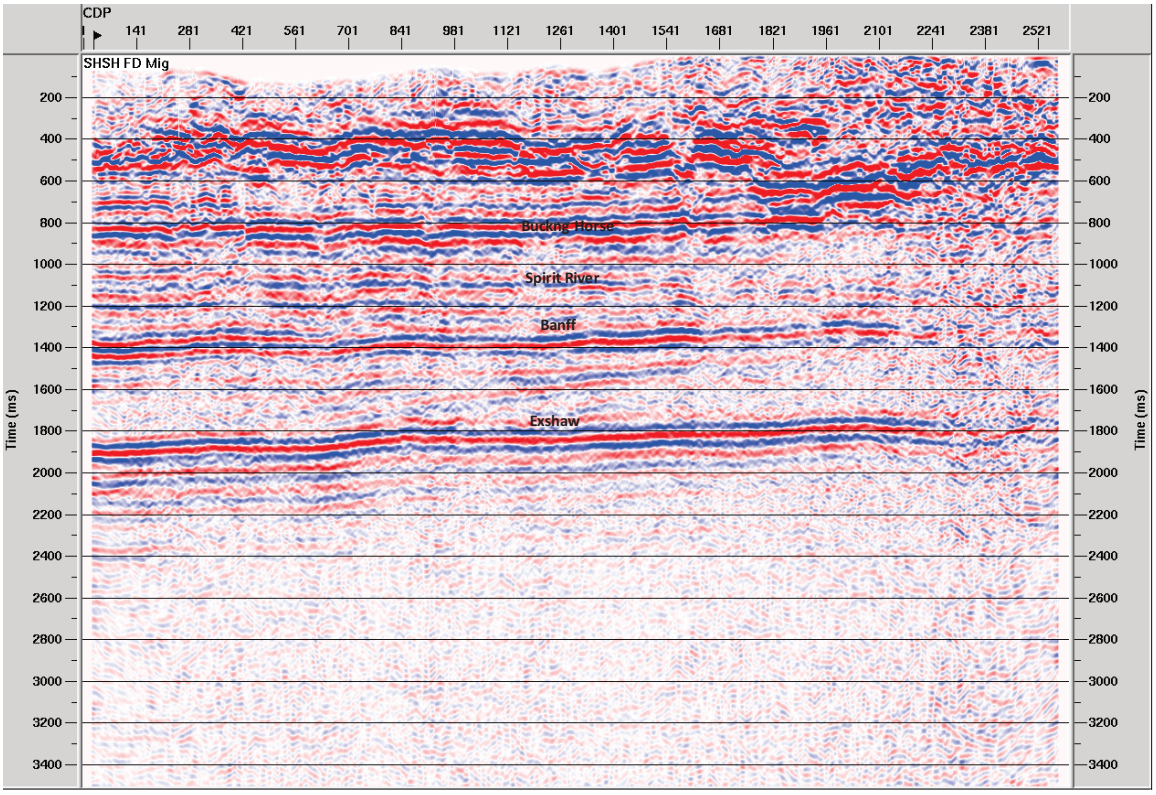

FIG 31. SH section after post-stack migration

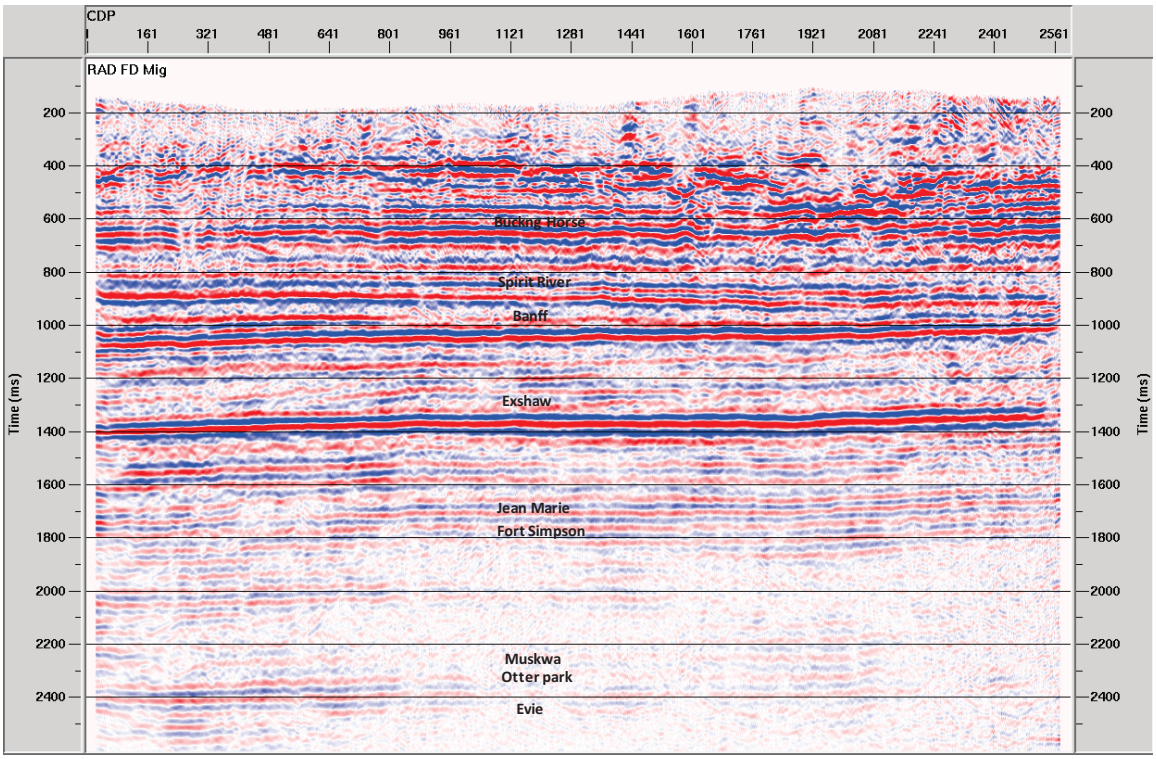

FIG. 32. PS section after post-stack migration

CONCLUSIONS

- Both depth sections, from compressional and shear data, show the channel confirming its existence that was indicated by an electromagnetic (EM) survey acquired in the area.

- The shear data was difficult to analyse from shot 310 to 355 because there were not enough first break times coming from the second refractor. The plus-minus window cannot be defined under this condition so the analysis cannot be performed with confidence in this segment.

- The final model produced from the SH data shows three layers in the west part of the line and two layers to the east side of the profile. The presence of a channel is confirmed in the east side and a lateral velocity variation is obtained for the deeper layer, decreasing towards the east, probably as a result of the channel formation in this section.

- The model obtained from the P-V data shows only two layers, and the channel is also detected. Some difficulty was encountered when applying the plus-minus method on the P-V data due to not enough offsets. The second shot from the pair chosen for the analysis could not be located close to the first shot so that the reciprocal time can be read from the data. It was necessary to extrapolate to find this value.

- The difference in model between the two wave modes is due to higher sensibility of shear waves to changes in velocities.

- The static corrections times for S-H data gave higher values (negatives) than the static corrections times for P-V data as it is expected due to lower velocity of the S-waves. The ratio goes from 12 to 16 (S to P).

- It is very important to have well log information in order to validate seismic reflectors on the data. Compressional and shear sonic logs allow the calculation of Vp/Vs ratios needed to register compressional (PP) and shear (S) data. Registration is a key element for joint interpretation of multiple image components (PP and PS images). Both data modes were tied to depth using synthetic seismograms derived from well logs.

- GLI method and the plus-minus method give a different near-surface model for the S-wave data because the GLI method forces continuous layers along the profile while the plus-minus method gives the flexibility of changing analysis windows depending on data changes. Data changes reflect changes in the sub-surface like the pinching out of a layer.

ACKNOWLEDGEMENTS

We would like to thank all CREWES sponsors for their support, the faculty staff and computer technicians in the CREWES project for all their help, Nexen for allowing us to show the results of this project. To Sensor for providing the results of their processing.

REFERENCES

Al Dulaijan, 2008, Near-surface characterization using seismic refraction and surface-wave methods: M.Sc. Thesis, University of Calgary

Cox, M., 1999, Static corrections for seismic reflection surveys: Society of Exploration Geophysicists

Dufour, J., 1996, Refraction statics analysis of P-S Seismic data using the plus-minus time analysis method: M. Sc. Thesis, Univ. of Calgary

Hagedoorn, J. G., 1959, The plus-minus method of interpreting seismic refraction sections: Geophysical prospecting, 7, 158-181.

Lawton, D.C., 1990, A 9-component refraction seismic experiment: Canadian journal of exploration geophysicist, **25**, Nos. 1&2, 7-16

Martin, F., 2002, First breaks analysis for 3D shear seismic refraction statics, EAGE 64th Conference & Exhibition

Morrow, D., Zhao, M., and Stasiuk, L.D., 2002, The gas bearing Devonian Presqu'ile Dolomite of the Cordova embayment region of British Columbia, Canada: Dolomitization and the stratigraphic template: AAPG Bulletin, **86**, No. 9, 1609-1638

Parry, D.G. and Lawton, D.C., 1993, Near surface characterization using a 9-component refraction survey: Cochrane, Alberta, CREWES Research Report, **5**

Petrel Robertson Consulting Ltd., 2003, Exploration Assessment of Deep Devonian Gas Plays, Northeastern British Columbia

Roche, S., Wagaman, M., and Watt H., 2005, Anadarko basin survey shows value of multicomponent acquisition: First Break, **23**, 43-51.

Sheriff, R.E., 1991, Encyclopedic dictionary of exploration geophysics: Society of Exploration Geophysicists

Simmons, J. L., Backus, and M. M., 1999, Radial-Transverse (SV-SH) coordinates for 9-C 3-D seismic reflection data analysis. Expanded Abstracts

Tatham, R.H., and McCormack, M. D., 1991, Multicomponent seismology in petroleum exploration: Society of Exploration Geophysicists